07

Gradient layers in a four-component Al−Ga−As−Sn system growth by liquid-phase epitaxy

© N.S. Potapovich, V.P. Khvostikov, O.A. Khvostikova, A.S. Vlasov

Ioffe Institute,
194021 St. Petersburg, Russia
e-mail: nspotapovich@mail.ioffe.ru

Received July 5, 2023
Revised August 23, 2023
Accepted August 25, 2023

The growth of thick (more than 50 μm) $Al_xGa_{1-x}As$ gradient layers in the Al−Ga−As−Sn system has been modeled. Sn-doped $Al_xGa_{1-x}As$ layers up to 85 μm thick were obtained by liquid-phase epitaxy. The obtained experimental profiles of the $Al_xGa_{1-x}As$ composition gradient satisfy the used theoretical model for the cases of growth from a limited volume of a solution−melt.

Keywords: Liquid phase epitaxy, AlGaAs, phase equilibrium, photovoltaic cell, gradient layers.

DOI: 10.61011/TP.2023.10.57454.168-23

Introduction

Gradient heterostructures based on thick (more than 50 μm) epitaxial layers $Al_xGa_{1-x}As$ with a smooth change in composition are currently used both for photovoltaic receivers with lateral radiation input [1–5], and for LED structures [6,7]. The configuration of side-input photovoltaic devices has a number of advantages: it reduces optical and ohmic losses (since both contacts are solid and the entire photodetector surface is open) and allows increasing the maximum power of photoelectric conversion.

The main task in growing this type of structures and highly efficient devices based on them is to obtain the required change in the composition of the solid solution (band gap width and refractive index) by the thickness of the epitaxial layer. The evaluation of the possibility of obtaining the necessary composition gradient when growing layers $Al_xGa_{1-x}As$ from a gallium melt by liquid-phase epitaxy was considered in the literature both for cases of growth from a semi-infinite volume and for the case of growth from a fined volume [8,9], where the velocity of diffusion of components in the liquid phase to the interface of the phases exceeds many times the growth rate of the layer, i.e. no depletion of the solution — of the melt occurs. In the case of high epitaxy temperatures ($T > 850^\circ$C), in the absence of intentional doping, crystallization of *p*-type layers is observed at the initial stage of growth, and then an inversion of the conductivity type occurs when the epitaxy temperature decreases [10,11]. Tin (Sn) is widely used as a donor impurity for $Al_xGa_{1-x}As$ due to its low volatility, especially at high epitaxy temperatures $T = 900-950^\circ$C [12]. In this case, the level of doping of epitaxial layers can vary significantly in thickness with the same tin content in the growth melt due to depletion of Al in the liquid phase during prolonged growth [13,14]. The theoretical estimates found in the literature are in practice of little use for designing and creation of side-input photovoltaic devices if it is necessary to obtain thick gradient layers of $Al_xGa_{1-x}As$ *n*-type with a given variation of the composition in thickness and doping level.

The purpose of this work is to find theoretical and experimental distribution curves of the composition $Al_xGa_{1-x}As$ and the refractive index along the thickness of the epitaxial layer at different Sn content in the melt and to determine the optimal conditions (growth temperature, composition of the liquid phase) necessary for the crystallization of gradient layers $Al_xGa_{1-x}As$ of the specified thickness.

1. Experimental

Layers $Al_xGa_{1-x}As$ were grown by liquid phase epitaxy from gallium melt. Tin (Sn) was added to the liquid phase to obtain layers of *n*-type conductivity. The tin content varied from 0 to 0.2 mol.f. (molar fractions) in the melt. The melt homogenization was performed at 20°C above the temperature of the beginning of layer growth (T_0) during 50−60 min. The growing layer was crystallized on GaAs substrates of orientation (100) in a stream of purified hydrogen. The epitaxy temperature was measured using a Pt−Pt/Rh thermocouple with an accuracy of 1°C. Epitaxial growth of the layers was carried out in a piston-type graphite boat, where the melt is forced through a slot using a piston. This contributed to the mechanical purification of the melt from possible oxide films. The use of a piston boat with a limited melt height ($h = 1.5$ mm) made it possible to significantly reduce the effect of the diffusion rate of components to the phase interface on the growth rate and the composition of the gradient layer. The cooling rate of the melt solution during epitaxy varied from 0.5 to 1°C/min.

Two experimental samples were prepared to study the composition gradient over the thickness of AlGaAs (see table). The $Al_xGa_{1-x}As$ layers of tin-gallium and

Conditions for growing experimental samples

№ Sample	Melt 1	Melt 2	Start of Growth	End of growth
1	Sn = 15% $V \approx 0.5$°C/min	Sn = 0% $V \approx 0.5$°C/min	$T_0 = 935$°C XAlAs = 0.53	$T = 805$°C XAlAs ≤ 0.1
2	Sn = 15% $V \approx 0.5$°C/min	Sn = 0% $V \approx 1.0$°C/min	$T_0 = 935$°C XAlAs = 0.57	$T = 805$°C XAlAs ≤ 0.1

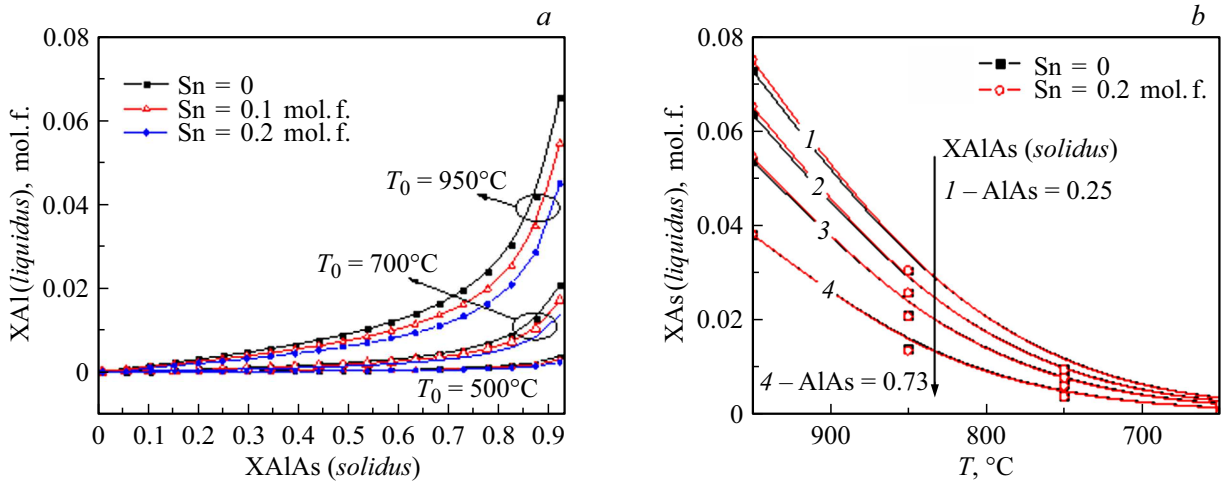

Figure 1. Calculated liquidus and solidus curves: *a* — dependence of the aluminum content in the liquid phase on the composition of the solid solution for different temperatures and the tin content in the solution–melt; *b* — the dependence of the arsenic content in the liquid phase on the temperature for different tin content in the solution–melt and different composition of the solid solution.

gallium melts were crystallized sequentially on a GaAs substrate. It is necessary to use two melts, since it is impossible to obtain gradient layers with a smooth change in composition ($x = 0.55-0.1$) without jumps in layer resistance from one growth melt [14–16]. The concentration of the growing layer strongly depends on the composition (XAlAs) in case of doping a solid solution $Al_xGa_{1-x}As$ with tin. The level of doping of the layer sharply dips in compositions $x = 0.35-0.4$. For this reason, the samples crystallized from two melts: 1) with a high tin content to obtain the required level of doping *n*-type, 2) without tin to avoid jumps in the layer resistance of the gradient layer [15,16].

Experimental values of the composition (x) of the solid solution $Al_xGa_{1-x}As$ were determined using the Raman spectroscopy method. The spectra were measured in the geometry of backscattering from the edge. The excitation was carried out by a 532nm laser through a lens with a magnification of 80×. The diameter of the spot on the sample surface was $\sim 1.5\,\mu$m. Scanning was carried out using micrometric movement in the direction of growth.

2. Theoretical part

In the case of growing a three-component solid solution $Al_xGa_{1-x}As$ from a multicomponent solvent (Ga + Sn) with an additional component that is not part of the solid phase, the phase equilibrium can be represented as

$$\langle\{Al_y(Ga_{1-a} + Sn_d)_{1-y}\}_{1-z}As_z\rangle liquidus = \langle Al_xGa_{1-x}As\rangle solidus.$$

Changes of the composition of the liquid phase during forced cooling are described by differential equations using the Pfann approximation. In this approximation, the linear dimensions of the growing layer are many times greater than its thickness, there is no diffusion in the solid phase, the solidified layers are no longer mixed, the diffusion rate in the liquid phase is many times higher than the growth rate of the layer (complete mixing) and the degree of supersaturation of the liquid phase, providing epitaxial growth, is so small that the concentrations of components in the growing layers of the solid phase determined by the equilibrium state diagram [17]:

$$dX^L_{Al}/(X^S_{Al} - X^L_{Al}) = dX^L_{As}/X^S_{As} - X^L_{As}.$$

The following differential equation with the initial condition $X^L_{Al} = X^L_{Al0}$ for $T = T_0$ can be obtained using the Pfann equation:

$$dX^L_{Al}/dT = dX^L_{As}/dT\,[(0.5x\text{AlAs} - X^L_{Al})/(0.5 - X^L_{As})], \quad (1)$$

where xAlAs, X^L_{As} and dX^L_{As}/dT are from the liquidus curves and 1).

The theoretical isotherms of liquidus and solidus were determined based on the model of quasi-regular solutions for $T = 950-500^{\circ}$C using equations given in [13,14]. There was a noticeable shift of phase equilibria (relative to the system Al−Ga−As) since the amount of tin required for doping was quite large and amounted to 0.2 mol.f. in solution in the melt, Al−Ga−As. The addition of the alloying component Sn does not lead to a change in the solid phase, and when modeling isotherms, only the activity coefficients of γ_i components in the liquid phase change. Fig. 1 shows that the introduction of tin at concentrations 0.1 and 0.2 mol.f. significantly reduces the equilibrium concentration of aluminum in the liquid phase, especially at high temperatures (950−700°C).

If we consider the case where the layer $Al_xGa_{1-x}As$ is grown from a three-component melt under the condition $X^L_{Ga} \approx 1$, then it is possible to use simplified formulas for the liquidus isotherm:

$$X^L_{As} = K(T)C(T)/\left(C(T) + X^L_{Al}\right),$$

$$K(T) = k_1 \exp(k_2/T), \tag{2}$$

$$C(T) = c_1 \exp(c_2/T). \tag{3}$$

Here k_1, k_2, c_1, c_2 — parameters of the simplified model, which are combinations of a much larger number of model parameters of a more general model of quasi-regular solutions.

Then the differential equation (1) has the following form

$$\frac{dX^L_{Al}}{dT} = \frac{(x\mathrm{AlAs} - 2X^L_{Al})[dK/dTC^2 + dK/dTCX^L_{Al} + dC/dTKX]}{(C + X^L_{Al} - 2KC)(C + X^L_{Al}) + KC(x\mathrm{AlAs} - 2X^L_{Al})}. \tag{4}$$

To obtain calculated composition gradient curves by the thickness of the growth layer, it is necessary to determine the thickness of the layer at each moment of the epitaxial process. It is possible to use a simplified formula for determining the thickness of the epitaxial layer without taking into account the diffusion coefficients of the components for the case when the epitaxial layer is grown at sufficiently low cooling rates from a growth melt limited in thickness (i.e., there is no depletion of the melt solution at the growth boundary of the epitaxial layer). If an equilibrium state is maintained at each moment of the process at the growth boundary, then the layer thickness is determined from the condition that the number of atoms in the solid is equal to the number of atoms that left the melt [18]:

$$d_{\max} = \rho_1 Msh/(\rho s A_1)[X(T_0)/N(T_0) - X(T)/N(T)],$$

where ρs and Ms — density and molecular weight of the solid layer; ρ_1 and A_1 — density and atomic weight of the solvent, h — height of the growth solution− of the melt.

3. Findings and discussion

The study of changes in the concentration of aluminum during a single technological process was carried out on the basis of a differential equation (4) taking into account the equations (2) and (3) and theoretical liquidus isotherms for the case when $X^L_{Ga} \approx 1$ can be used to estimate the gallium content in the melt. The fourth order Runge−Kutta method was used to solve the equation, the parameters of the simplified model for the system Al−Ga−As (for Sn = 0) are taken from [8,9]: $k_1 = 3600$; $k_2 = -12930$; $c_1 = 2.614$; $c_2 = -6800$. The change of the concentration of aluminum in the liquid phase during the growth of gradient epitaxial layers in the temperature range from 950 to 500°C was calculated on the basis of the differential equation (1) for cases when the gallium content in the melt was 0.9 mol.f. and less.

Fig. 2 shows that at a low initial concentration of aluminum in the liquid phase — less than 0.01 mol.f., aluminum depletion occurs already at temperatures 800−850°C, which leads results in the growth of inhomogeneous epitaxial structures containing an extremely low aluminum content layer on the surface.

A noticeable decrease of the equilibrium concentration of aluminum in the liquid phase and, accordingly, an increase of the aluminum distribution coefficient was observed for cases when tin was added to the gallium solution−melt (Fig. 2, *b*). Fig. 2, *b* shows that the rate of depletion of components in the liquid phase is faster with an increase of the proportion of tin in the solution−melt in case of a prolonged crystallization with a decrease in temperature, which should lead to a noticeable decrease of the final maximum thickness of the epitaxial layer. Nevertheless, there was no noticeable change (decrease) of the thickness of the layer in practice, taking into account the simultaneously increasing aluminum distribution coefficient when growing from melts containing tin.

AlGaAs gradient layers with a thickness up to 85 μm were grown based on the performed calculations (see table). The cooling rate in the second part of the epitaxy doubled in the case of sample №2, which was performed to check the effect of the cooling rate of the growth melt on the final layer thickness. The initial parameters for modeling (XAlAs, T_0) were selected consistent with the grown samples for comparison of the experimental profile of the solid solution composition with the calculated values. The distribution was calculated taking into account the thickness of the growth solution−melt and was assumed to be 1 and 1.5 mm (Fig. 3).

The experimental data obtained and the results of theoretical modeling show a fairly good consistency for the sample №1 over the entire thickness up to 80 μm. However, there is a strong discrepancy between the theoretical and experimental data in the case of the second sample. The thickness of the grown layer turned out to be noticeably less than predicted, only 65 μm. This can be explained by an increase of the cooling rate of the grown structure

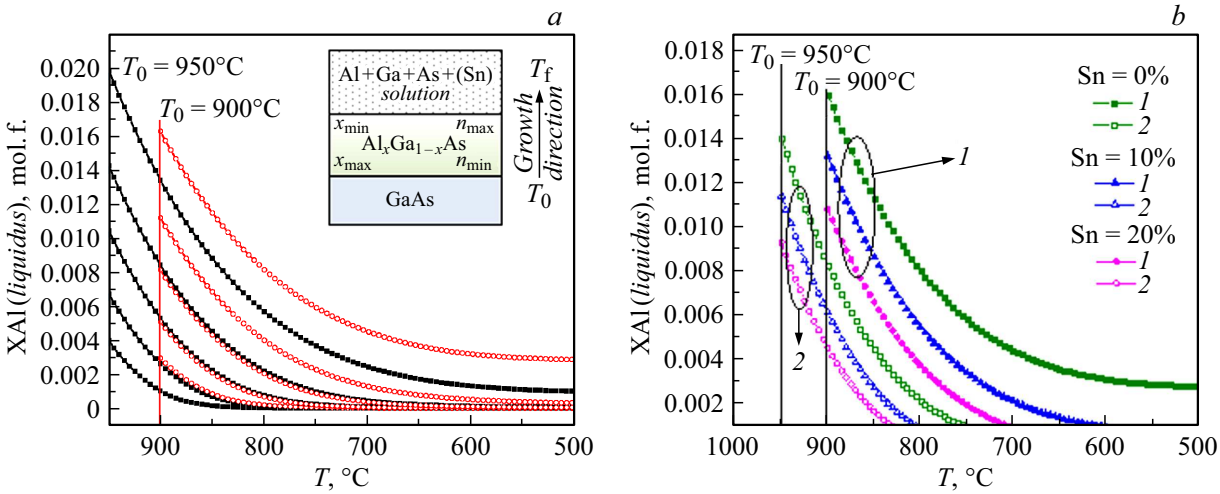

Figure 2. Change in the concentration of aluminum in the liquid phase during the growth of AlGaAs gradient layers: *a* — from pure gallium under various conditions of the beginning of epitaxy (temperature T_0, composition of the liquid phase $X_0^L(\mathrm{Al})$); *b* — at different contents of tin (Sn) in the growth melt of gallium, where *1* — XAlAs = 0.73 and $T_0 = 900°\mathrm{C}$; *2* — XAlAs = 0.63 and $T_0 = 950°\mathrm{C}$.

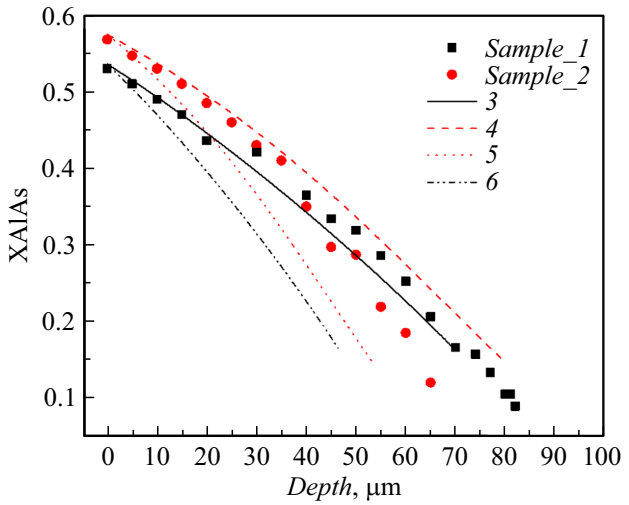

Figure 3. Change of the composition of the solid solution by thickness: *1, 2* — experimental points; *3, 4* — calculated curves in case of a growth from a melt with a height of 1.5 mm; *5, 6* — calculated curves in case of a growth from melt with a height of 1 mm.

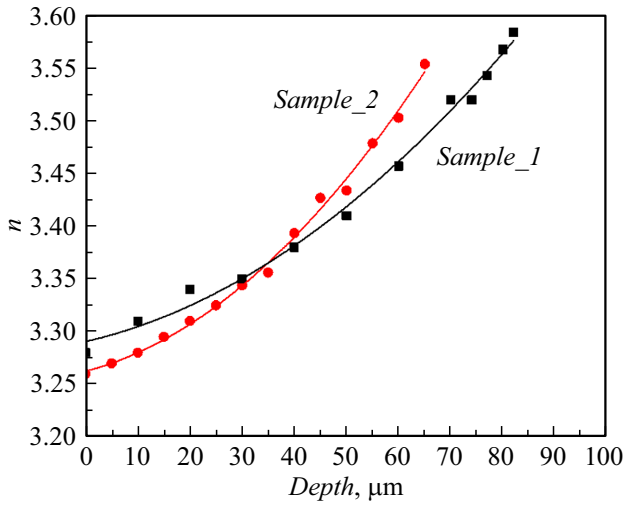

Figure 4. Variation of the refractive index along the thickness of the epitaxial layer calculated for the wavelength of incident radiation $\lambda = 850$ nm.

after the start of growth from the second melt, since the calculated modeling did not take into account the diffusion rates of the components (Al and As) in the gallium melt. Apparently, the thickness of the grown layer is limited by the diffusion rate of the melt components when the cooling rate $V_{\mathrm{cool}} \geq 1°\mathrm{C/min}$ is reached at epitaxy temperatures 870°C and below, and the resulting thickness of the grown layer turns out to be lower at a higher cooling rate. The theoretical curve *4* in this case describes the maximum possible layer thickness at the given initial parameters.

The gradient layers developed in the present work are necessary for the creation of side-input photovoltaic converters ($\lambda = 850$ nm). The waveguide (gradient) layer $\mathrm{Al}_x\mathrm{Ga}_{1-x}\mathrm{As}$ in such devices redirects light rays to the active region of the photoelectric converter by changing the refractive index of the layer from the substrate to the surface.

The refractive indices were calculated depending on the composition of the epitaxial layer (Fig. 4) for the epitaxial gradient layers obtained in the work [19]. The changes of the refractive index in the obtained samples correspond to an exponential profile (Fig. 4). It was the exponential profile of the distribution of the refractive index over the thickness of the waveguide layer that had the maximum irradiation and the largest area of $p-n$-transition for full absorption in the region close to the photodetector according to the modeling in [2]. Such a refractive index profile is preferable for high-power AlGaAs/GaAs laser converters.

Conclusion

Modeling and comparative analysis of changes of the aluminum content during crystallization of the gradient layer $Al_xGa_{1-x}As$ in the system Al–Ga–As–Sn (for Sn from 0 to 20 mol.f.) in the temperature range 950–500°C. Gradient layers $Al_xGa_{1-x}As$ $(0.6 \geq x \geq 0.1)$ up to 85 μm thick were grown using liquid phase epitaxy method based on the calculations performed with a change in the refractive index from 3.26 at the boundary with the substrate up to 3.58 on the surface of a solid solution. A smooth gradient of the refractive index, varying exponentially in the AlGaAs/GaAs heterostructure, is necessary for a uniform distribution of radiation incident on the edge face of the photoconverter over the entire area of the $p-n$ junction. The results obtained can be used to create highly efficient photovoltaic converters with lateral input of high-power laser radiation and infrared LEDs.

Acknowledgments

This study was supported by a grant from the Russian Science Foundation, project №22-19-00057, https://rscf.ru/project/22-19-00057/.

Conflict of interest

The authors declare that they have no conflict of interest.

References

[1] M. Perales, M. Yang, Ch. Wu, Ch. Hsu, W. Chao, K. Chen, T. Zahuranec. In: Proc. SPIE 9733, High-Power Diode Laser Technology and Applications XIV, 97330U, 97330U-1 (2016). DOI: 10.1117/12.2213886
[2] V.P. Khvostikov, P.V. Pokrovskiy, O.A. Khvostikova, A.N. Panchak, V.M. Andreev. Tech. Phys. Lett., **44**, 776 (2018) DOI: 10.1134/S1063785018090079
[3] A. Panchak, V. Khvostikov, P. Pokrovskiy. Opt. Laser Technol., **136**, Paper N106735 (2021). DOI: 10.1016/j.optlastec.2020.106735
[4] V.P. Khvostikov, A.N. Panchak, O.A. Khvostikova, P.V. Pokrovskiy. IEEE Electron Device Lett., **43**, 1717 (2022). DOI: 10.1109/LED.2022.3202987
[5] B. Kashyap, A. Datta. IEEE Trans. Electron Devices, **64** (6), 2564 (2017). DOI: 10.1109/TED.2017.2692267
[6] V. Zinovchuk, O. Malyutenko, V. Malyutenko, A. Podoltsev, A. Vilisov. J. Appl. Phys., **104**, Paper N033115 (2008). DOI: 10.1063/1.2968220
[7] H. Kitabayashi, K. Ishihara, Y. Kawabata, H. Matsubara, K. Miyahara, T. Morishita, S. Tanaka. SEI Tech. Rev., **72**, 86 (2011). https://sumitomoelectric.com/sites/default/files/2020-12/download_documents/72-12.pdf
[8] M.R. Dombrugov. Microsyst. Electron. Acoust., **24** (1), 6 (2019). DOI: 10.20535/2523-4455.2019.24.1.160164
[9] V.A. Ilyukhin, S.Yu. Karpov, E.L. Portnoy, D.N. Tretyakov. Pisma v ZHTF, **4** (11), 629 (1978) (in Russian).
[10] X. Zhao, K.H. Montgomery, J.M. Woodall. J. Electron. Mater., **43** (11), 3999 (2014). DOI: 10.1007/s11664-014-3340-x
[11] V. Khvostikov, O. Khvostikova, N. Potapovich, A. Vlasov, R. Salii. Heliyon, **9** (7). e18063 (2023). DOI: 10.1016/j.heliyon.2023.e18063
[12] A. Saragan. *Physical and Chemical Vapor Deposion in Nanofabrication.* Ch. 3. (CRC Press, 2016), DOI: 10.1201/9781315370514
[13] H.C. Casey, M.B. Panish. *Heterostructure Lasers* (Academic Press, 1978), DOI: 10.1016/B978-0-12-163102-4.50009-9
[14] M.B. Panish. J. Appl. Phys., **44**, 2667 (1973). DOI: 10.1063/1.1662631
[15] K. Kaneko, M. Ayabe, N. Watanabe. Inst. Phys. Conf. Ser., **33a**, 216 (1977).
[16] M.C. Wu, Y.K. Su. J. Crystal Growth, **96**, 52 (1989). DOI: 10.1016/0022-0248(89)90275-3
[17] W.G. Pfann. *Zone Melting* (Wiley, 1958). DOI: 10.1107/S0365110X5900130X
[18] E. Kuphal. Appl. Phys., **A52**, 380 (1991). DOI: 10.1007/BF00323650
[19] S. Adachi. *III–V Ternary and Quaternary Compounds. Springer Handbook of Electronic and Photonic Materials* (Springer, 2017), p. 725–741. DOI: 10.1007/978-3-319-489339_30

Translated by Ego Translating